CALIBRATION UNIT FOR HYDROPHONE LINE ARRAYS

NAVAL UNDERSEA CENTER
SAN DIEGO, CALIFORNIA

NOVEMBER 1976

NUC TP 539

CALIBRATION UNIT FOR HYDROPHONE LINE ARRAYS

by

Joseph L. Percy

UNDERSEA SURVEILLANCE DEPARTMENT

November 1976

NAVAL UNDERSEA CENTER, SAN DIEGO, CA. 92132

AN ACTIVITY OF THE NAVAL MATERIAL COMMAND

R. B. GILCHRIST, CAPT, USN
Commander

HOWARD L. BLOOD, PhD
Technical Director

ADMINISTRATIVE INFORMATION

The array calibration unit described in this report was designed, constructed, and initially used from December 1971 to February 1972 by members of the Ocean Acoustics Division. The work was sponsored by the Advanced Research Project Administration under ARPA Order 2001. The remainder of the work covered by this report, though unsponsored, was completed by a member of the System Concepts and Analysis Division, who worked at it intermittently from August 1973 to September 1976.

This report was written, first, to apprise NUC personnel using this calibration unit of corrections to be made to their calibrated receiving sensitivity curves, secondly, to inform those not using this unit of its presence at NUC, and last, to aid those who wish to design a similar unit.

L. K. Arndt and R. A. Wagstaff reviewed this report for technical accuracy.

The author wishes to express appreciation to C. E. Hansen for his helpful suggestions on the construction of the calibration unit.

Released by
M. R. Akers, Head
System Concepts and
Analysis Division

Authorized by
H. A. Schenck, Head
Undersea Surveillance
Department

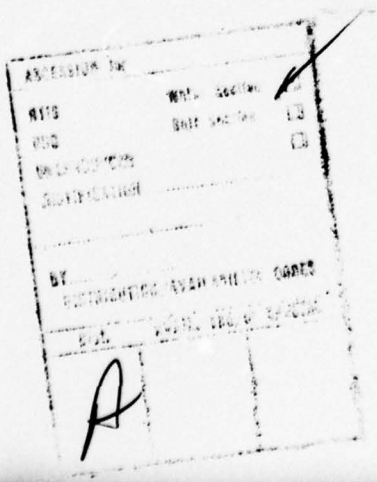

UNCLASSIFIED

SECURITY CLASSIFICATION OF THIS PAGE *(When Data Entered)*

REPORT DOCUMENTATION PAGE		READ INSTRUCTIONS BEFORE COMPLETING FORM
1. REPORT NUMBER NUC TP 539	2. GOVT ACCESSION NO.	3. RECIPIENT'S CATALOG NUMBER
4. TITLE *(and Subtitle)* CALIBRATION UNIT FOR HYDROHPONE LINE ARRAYS		5. TYPE OF REPORT & PERIOD COVERED Final Report; Dec 71 to Sep 76
		6. PERFORMING ORG. REPORT NUMBER
7. AUTHOR(s) Joseph L. Percy		8. CONTRACT OR GRANT NUMBER(s)
9. PERFORMING ORGANIZATION NAME AND ADDRESS Naval Undersea Center San Diego, Calif. 92132		10. PROGRAM ELEMENT, PROJECT, TASK AREA & WORK UNIT NUMBERS ARPA Order 2001
11. CONTROLLING OFFICE NAME AND ADDRESS Naval Material Command Washington, D.C. 20360		12. REPORT DATE Nov. 1976
		13. NUMBER OF PAGES 37
14. MONITORING AGENCY NAME & ADDRESS(if different from Controlling Office)		15. SECURITY CLASS. (of this report) Unclassified
		15a. DECLASSIFICATION/DOWNGRADING SCHEDULE

16. DISTRIBUTION STATEMENT *(of this Report)*

Approved for public release; distribution unlimited.

17. DISTRIBUTION STATEMENT *(of the abstract entered in Block 20, if different from Report)*

18. SUPPLEMENTARY NOTES

19. KEY WORDS *(Continue on reverse side if necessary and identify by block number)*

Line Array, Acoustic Calibration, Phase Differences,
Spherical Spreading, Image Interference

20. ABSTRACT *(Continue on reverse side if necessary and identify by block number)*

A calibration method applicable for long line array segments is investigated.

A theoretical discussion is given on the corrections required to modify measured receiver sensitivity curves obtained by use of a simple calibration device. These corrections are for the effects of phase difference, spherical spreading, and image interference. Curves are presented from which the calibration corrections can be obtained for array segments of 3 to 24 layers and for calibration units having radii to 3 meters and covering a frequency spectrum up to 10 kHz.

DD FORM 1 JAN 73 1473 EDITION OF 1 NOV 65 IS OBSOLETE

UNCLASSIFIED

SECURITY CLASSIFICATION OF THIS PAGE *(When Data Entered)*

20. Continued

A calibration unit constructed at NUC in 1972 is described, and test results using this unit are presented. Errors associated with this unit due to phase differences are less than -0.1 dB below 1 kHz, spherical spreading losses are no more than -0.2 dB, and image interference effects range from 0 dB at 10 Hz to 0.1 dB at 1 kHz, indicating that no correction to the measured receiver sensitivity is required for this calibration unit.

SUMMARY

Problem

Devise a method of calibrating acoustic hydrophone line array segments that are about 100 meters long.

Results

A calibration method applicable for long line array segments is investigated.

A theoretical discussion is given on the corrections required to modify measured receiver sensitivity curves obtained by use of a simple calibration device. These corrections are for the effects of phase difference, spherical spreading, and image interference. Curves are presented from which the calibration corrections can be obtained for array segments of 3 to 24 layers and for calibration units having radii to 3 meters and covering a frequency spectrum up to 10 kHz.

A calibration unit constructed at NUC in 1972 is described, and test results using this unit are presented. Errors associated with this unit due to phase differences are less than −0.1 dB below 1 kHz, spherical spreading losses are no more than −0.2 dB, and image interference effects range from 0 dB at 10 Hz to 0.1 dB at 1 kHz, indicating that no correction to the measured receiver sensitivity is required for this calibration unit.

Recommendation

This type of calibration unit should be used for the calibration of all future Navy line array segments.

CONTENTS

Summary iii
Introduction 1
Line Array Calibration Method 2
    Calibration Requirements 2
    Design Considerations 3
        Phase Differences 3
        Spherical Spreading 5
        Image Interference 6
        Calibration Corrections 8
NUC Calibration Unit 15
    Unit Description 15
    Test Results 15
        Phase Differences for NUC Unit 15
        Spherical Spreading for NUC Unit 16
        Image Interference for NUC Unit 16
        Calibration Corrections for NUC Unit 16
Summary of Results 23
Conclusions 24
Recommendations 24
Appendix: Computer Programs for HP 9830 25

INTRODUCTION

During the NUC Forward Area Sonar Research cruise in 1969 (FASOR III), a short line array having an active hydrophone section of 1.7 meters was used for acoustic propagation studies. This short array was calibrated at Transdec (the NUC test calibration facility) by suspending the active section below a submerged beam within the test facility and using the substitution method of calibration.

This technique worked for a short array, but could not be used for an array segment over 100 meters long. In fact, a long array segment had never been calibrated.

In December 1971, the Naval Undersea Center (NUC) conducted a series of successful acoustic noise tests in Exuma Sound, the Bahamas, using a leased long linear hydrophone array. The results of these tests were instrumental in establishing the Large Aperture Marine Basic Data Array (LAMBDA) project at NUC, and this introduced NUC into the field of long line arrays.

The task then was to devise a method for calibrating long line array segments.

In January 1972, NUC designed and constructed a calibration unit for hydrophone line arrays. It is the purpose of this report to describe and evaluate this unit for present and future users: for present users, to apprise them of corrections they should make to their calibrated receiving sensitivity curves, and for future users, to inform them of the unit's existence and, more important, its capabilities.

The report is divided basically into two parts. In the first part there will be a general discussion of the method of calibrating hydrophone line arrays. In the second part, NUC's calibration unit will be described and evaluated on the basis of its test results.

LINE ARRAY CALIBRATION METHOD

Calibration Requirements

The history of hydrophone calibration methods is a history of facilities capable of performing the various types of calibrations that have been applied to hydrophones to produce a value called the receiving response, or sensitivity, of the hydrophone.

The various methods of calibration, whether absolute, reciprocal, substitution, or the like, furnish a value of sensitivity, representing the characteristics of the hydrophone being tested. However, these methods, accepted by the scientific community for omnidirectional hydrophones, fail when applied to the receiving response of a directional line array.

A line array is defined as a group of hydrophones in a one-dimensional line. Other factors, such as number of hydrophones within a group, spacing between hydrophones or between groups, and operational frequency range, characterize the line array under consideration.

The line array can be either linear or tapered. Linear arrays have repeatable spacings between hydrophone groups or elements, while tapered arrays have a spatially different separation between elements in the hydrophone group. In a tapered array a chosen point within the group represents the phase center of the group; that is, an acoustic wave traveling from either end of the group will arrive at the acoustic phase center in phase.

The difficulty in calibrating a line array is primarily with arranging the length of the array and the separation between the array and the transmitting source such that the acoustic signal from the transmitter arrives in phase at all hydrophone group centers simultaneously.

At high frequencies (10 kHz or greater), this problem becomes one of having a large enough tank to perform the experiment, as seen in Table 1.

Table 1. Far-field distances as a function of frequency.

Frequency, Hz	Range, m
1	3.75×10^4
10	3.75×10^3
100	3.75×10^2
1K	3.75×10^1
10K	3.75
100K	3.75×10^{-1}

At low frequencies, the problem becomes one of performing the experiment over many miles of lake or ocean where the receiving array and transmitting transducer must be at the proper depth in isovelocity water to receive an acoustic signal that has not been interfered with by multipath arrivals.

Before the introduction of the NUC calibration unit, the array had to be placed in the far field of the acoustic source. This range is given as

$$R > L^2/\lambda \tag{1}$$

where L is the length of the array and λ is the wavelength of the transmitted signal.

This equation can be expressed as

$$R > \frac{c(n-1)^2}{4} \cdot \frac{f}{f_0^2} \tag{2}$$

for a linear array having n element groups with spacings of $\lambda_0/2$, from which we have used $f_0 = c/\lambda_0$ as the half wavelength frequency, c as the velocity of sound in water, and f as a variable frequency.

This equation was used to devise Table 1 with $n = 11$, $c \approx 1500$ m/s and $f = f_0$.

It is seen from Table 1 that at low frequencies ($f < 100$ Hz), line arrays could not be calibrated with existing facilities.

Design Considerations

A line array coiled in a circle would have all hydrophones at an equal distance from a transmitter located at the center of the coil. This configuration allows all signals to arrive in phase at all hydrophones.

Line array segments, which make up the total line array, are usually around 50 to 100 meters long. This large size necessitates that the array be coiled in a helix and the problem then is to construct this helix so that the measured hydrophone sensitivity will not be adversely affected by phase differences, spherical spreading, and image interference.

Phase Differences. For a line array coiled in a helix, partially shown in Fig. 1, the output from the array is given by:

$$V_0 = \sum_{\ell=1}^{L} \sum_{m=1}^{M} V_{m\ell} \cdot e^{i\delta m\ell} \tag{3}$$

where we have L layers each having M hydrophones. $V_{m\ell}$ is the response of hydrophone m in layer ℓ, and $\delta_{m\ell}$ is the phase delay between these hydrophones.

For uniform hydrophone response, V, we have:

$$V_0 = MV\left(1 + 2 \cdot \sum_{\ell=3}^{L} e^{i\delta\ell}\right), \qquad \ell = 3, 5, 7, \ldots L \tag{4}$$

$$V_0 = 2MV\left(1 + \sum_{\ell=4}^{L} e^{i\delta\ell}\right), \qquad \ell = 4, 6, 8, \ldots L \tag{5}$$

and

$$\delta_\ell = \frac{2\pi}{\lambda}\left\{\left[\left(\frac{\ell-1}{2} \cdot d\right)^2 + R^2\right]^{1/2} - R\right\} \qquad \textit{odd or even } L$$

where

d is the diameter of the line array hose body

R is the radial distance from the center of the helix to the array

The error in sensitivity due to phase differences between hydrophones in the different layers within the helix can be determined from:

$$\text{Phase error} = 20 \log \left\{V_0/MV(1 + 2K)\right\} \tag{6}$$

$$= 20 \log \left\{\left(1 + 2\left[\left(\sum_{\ell=3}^{L} \cos\delta_\ell\right)^2 + \left(\sum_{\ell=3}^{L} \sin\delta_\ell\right)^2\right]^{1/2}\right)\Big/ (1 + 2K)\right\} \qquad \ell = 3, 5, 7, \ldots L \tag{7}$$

for an odd number of layers.

$$\text{Phase error} = 20 \log \left\{ V_\theta / 2MV(1+K) \right\}^{1} \tag{8}$$

$$= 20 \log \left\{ \left(1 + \left[\left(\sum_{\ell=4}^{L} \cos \delta_\ell \right)^2 + \left(\sum_{\ell=4}^{L} \sin \delta_\ell \right)^2 \right]^{1/2} \right) \Big/ (1+K) \right\} \qquad \ell = 4, 6, 8, \ldots L \tag{9}$$

for an even number of layers.

where

$$K = \sum_{\ell=3 \text{ or } 4}^{L} \tag{10}$$

ℓ = running index to account for the even or odd L hydrophones

Computer programs were written to evaluate these and the following equations, and are listed in the Appendix.

Design considerations have been given to include frequencies and number of layers far beyond the practical limit to show the onset of phase interference.

Figures 2 through 4 are presented to show the phase errors at 1, 5, and 10 kHz versus helix radii from 0.6 to 3 meters and for helixes from 3 to 17 and 3 to 24 layers and an array hose diameter of 9 cm. At high frequencies of 5 or 10 kHz, an interference pattern is established for a large number of layers, and the phase error oscillates about the −10 dB level. Layers greater than 17 were therefore omitted to avoid confusion of the sort seen in Fig. 4.

Phase errors were found to decrease with increasing radii.

Spherical Spreading. Spherical spreading losses due to the difference in separation between source transducer and reference hydrophone and source and array segment layer were derived similarly and are:

$$\text{Distance error} = 20 \log \left\{ \left(1 + 2R \sum_{\ell=3}^{L} \frac{1}{P_\ell} \right) \Big/ (1+2K) \right\}$$

$$\ell = 3, 5, 7, \ldots L \tag{11}$$

for an odd number of layers.

$$\text{Distance error} = 20 \log \left\{ \left(1 + R^* \sum_{\ell=4}^{L} \frac{1}{P_\ell} \right) \Big/ (1 + K) \right\}$$

$$\ell = 4, 6, 8, \ldots L \tag{12}$$

for an even number of layers.

where

$$P_\ell = \left\{ \left[\left(\frac{\ell - 1}{2} \right) \cdot d \right]^2 + R^2 \right\}^{1/2} \tag{13}$$

$$R^* = \left\{ \left(\frac{d}{2} \right)^2 + R^2 \right\}^{1/2} \tag{14}$$

Figure 5 illustrates the error in spherical spreading for helix radii from 0.6 to 3 meters and for a helix of 3 to 24 layers. Spherical spreading errors were found to decrease with increasing radii and to increase with increasing number of layers.

Image Interference. Image interference, or Lloyd mirror effect, must be taken into consideration whenever an acoustic source and receiver are near the surface or the bottom. This is due to constructive and destructive interference between the direct signal, the surface reflected signal, and the bottom reflected signal.

If we extend the theory as given by Urick* to include bottom reflected sound and spherical spreading, we can generate another family of curves to show the losses due to image interference.

Let

$$p_3 = \frac{A}{R_3} \sin(\omega t) \tag{15}$$

$$p_1 = -\mu_1 \frac{A}{R_1} \sin \omega(t + \tau_{13}) \tag{16}$$

$$p_2 = \mu_2 \frac{A}{R_2} \sin \omega(t + \tau_{23}) \tag{17}$$

* Urick, R. J. *Principles of underwater sound for engineers*, pp. 110–13. McGraw-Hill Book Co., 1967.

where p_3, p_1, and p_2 represent the pressures at a field point for the direct signal and the surface and bottom reflected signals, respectively (Fig. 6).

A is the source strength at the source point

μ_1 and μ_2 are the surface and bottom reflection coefficients

$$\tau_{13} = (R_1 - R_3)/c \tag{18}$$

$$\tau_{23} = (R_2 - R_3)/c \tag{19}$$

τ = time differences between the different arrivals

The combined pressure at a field point on one layer is given by

$$p = p_1 + p_2 + p_3 \tag{20}$$

and the intensity is given by the time average of the squared pressure over a half cycle as

$$I = \frac{\overline{p^2}}{\rho c} \tag{21}$$

$$= \frac{\overline{(p_1 + p_2 + p_3)^2}}{\rho c} \tag{22}$$

$$= \frac{1}{\rho c}\frac{2}{T}\int_0^{T/2} (p_1 + p_2 + p_3)^2 \, dt \tag{23}$$

where ρ = the density of water.

After performing the integration and introducing the average intensity at the field point due to the source alone as

$$I_0 = \frac{{p_3}^2}{2\rho c} = \frac{A^2}{2\rho c {R_3}^2} \tag{24}$$

we have

$$\frac{I}{I_0} = \left[1 + \mu_1^2 \left(\frac{R_3}{R_1}\right)^2 + \mu_2^2 \left(\frac{R_3}{R_2}\right)^2 + 2 R_3 \left\{ \frac{\mu_2 \cos(\omega\tau_{23})}{R_2} - \frac{\mu_1 \cos(\omega\tau_{13})}{R_1} \right\} \right.$$

$$\left. - \frac{2 R_3^2 \mu_1 \mu_2}{R_1 R_2} \left\{ \cos(\omega\tau_{13}) \cos(\omega\tau_{23}) + \sin(\omega\tau_{13}) \sin(\omega\tau_{23}) \right\} \right] \quad (25)$$

Equation 25 thus shows the modification of the acoustic field due to image interference of the surface and bottom at a field point on one layer.

The total image error for all layers of the array segment is then

$$\text{Image error} = 10 \log \left[\frac{1}{L} \sum_{\ell=2}^{L} \frac{I}{I_0} \right]; \qquad \ell = 2, 4, 6, \ldots L \quad (26)$$

$$= 10 \log \left[\frac{1}{L} \sum_{\ell=3}^{L} 1 + \frac{I}{I_0} \right]; \qquad \ell = 3, 5, 7, \ldots L \quad (27)$$

Figures 7 through 11 show the changes in image error versus radii for the various even and odd layers at 1, 5, and 10 kHz. These values were obtained by considering all reflection coefficients as $\mu = 1$, and the calibration unit midway between surface and bottom. In all cases the trend is to increase image errors with increasing radii and increasing error for increasing number of layers at 1 kHz up to 12 or 13 layers, at which time the error decreases. At 5 kHz the error curves are fairly well grouped together, and at 10 kHz the curves diverge into two families of curves.

Calibration Corrections. In each instance of phase differences, radial spreading, and image interference, the value obtained for the measured receiving sensitivity of the array segment will have been reduced for all negative error terms and increased for those that were positive. To remedy this the corrected array receiver sensitivity for small errors is given algebraically by:

Corrected array sensitivity = Measured receiver sensitivity

- Phase error - Distance error

- Image error (28)

Measured receiver sensitivity of a hydrophone is obtained by the substitution method of calibration and is usually modified by image interference effects between the source transducer, the calibrated reference hydrophone, the water surface, and the bottom. For frequencies below 1 kHz and for near-normal incidence from surface and bottom, the assumption $\mu = 1$ is quite valid. Under these circumstances, if the source and reference hydrophone are midway between surface and bottom, Eq. 25 shows that $I/I_0 = 1$ and this extra modification does not need to be made.

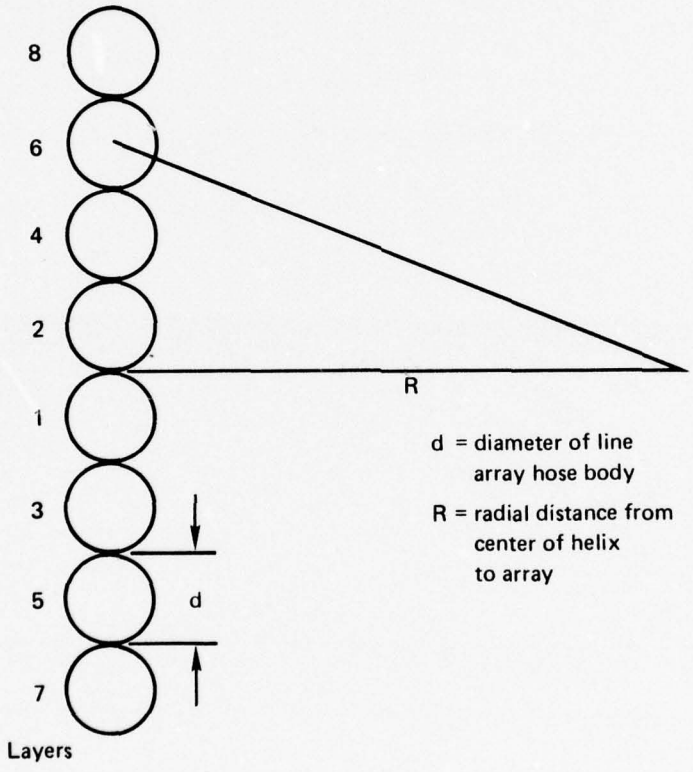

Figure 1. Layer counting, one side of helix.

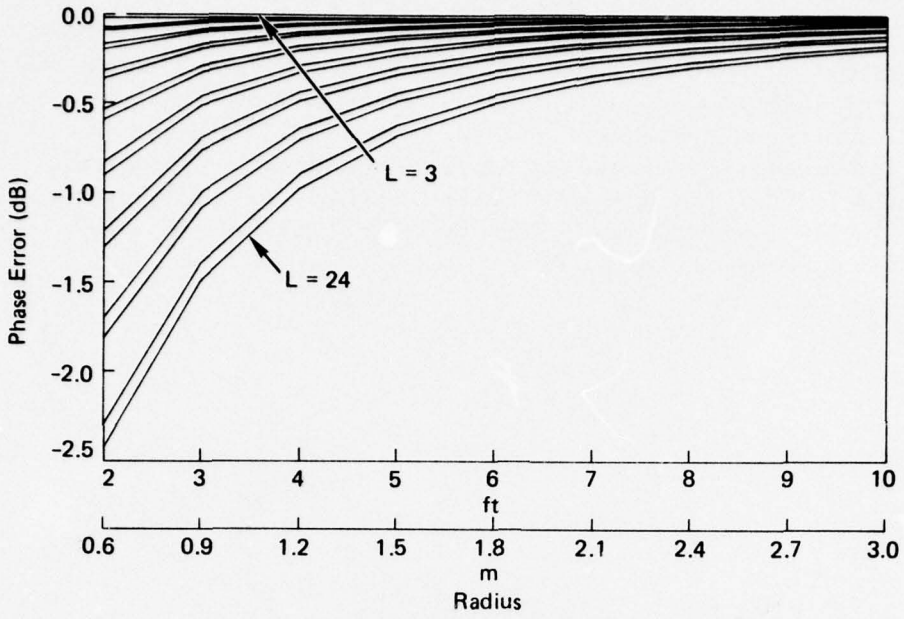

Figure 2. Phase error versus radius at 1 kHz.

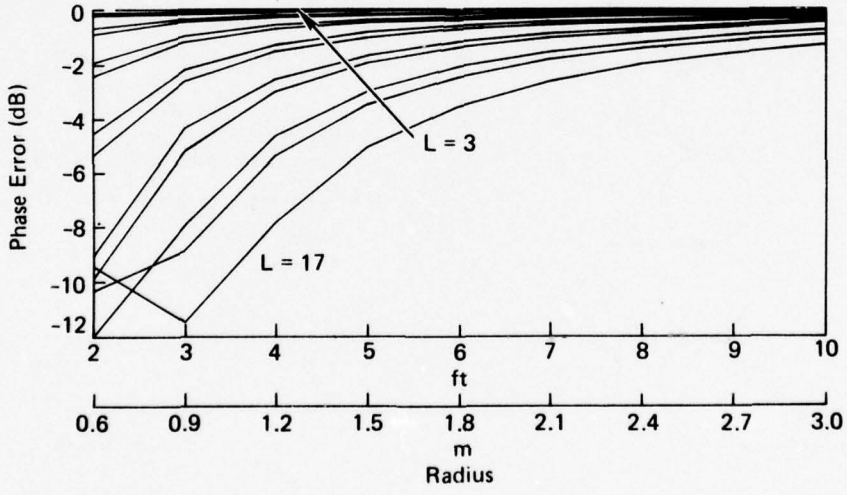

Figure 3. Phase error versus radius at 5 kHz.

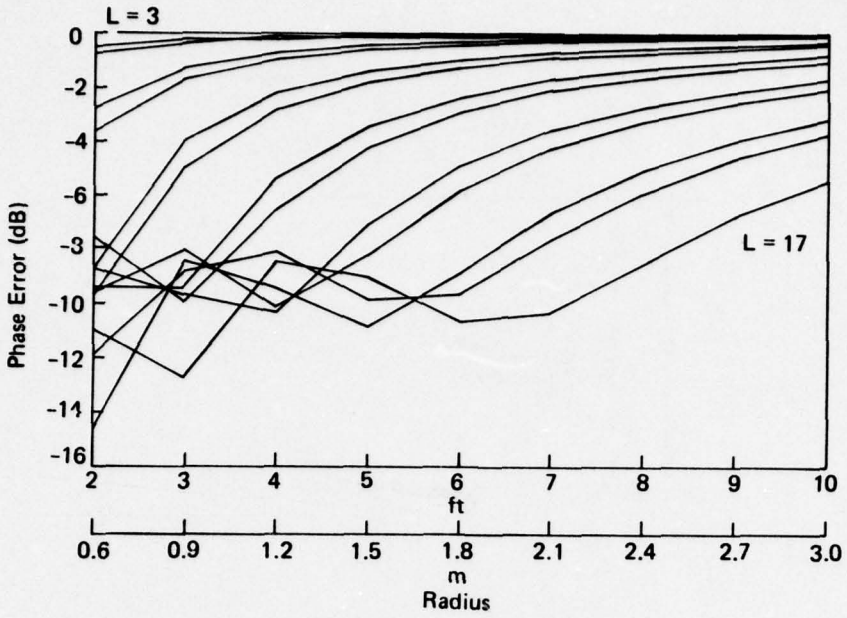

Figure 4. Phase error versus radius at 10 kHz.

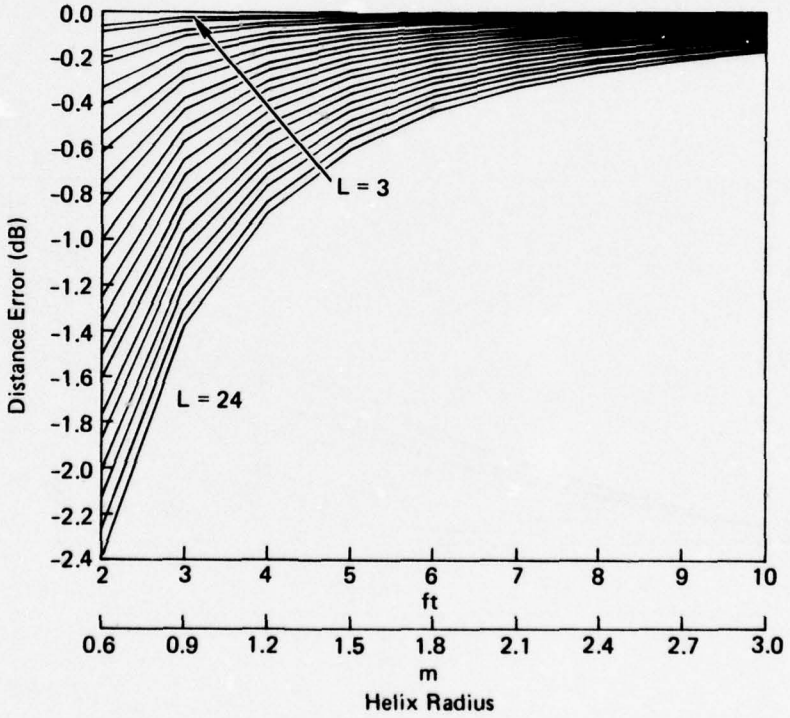

Figure 5. Distance error versus helix radius.

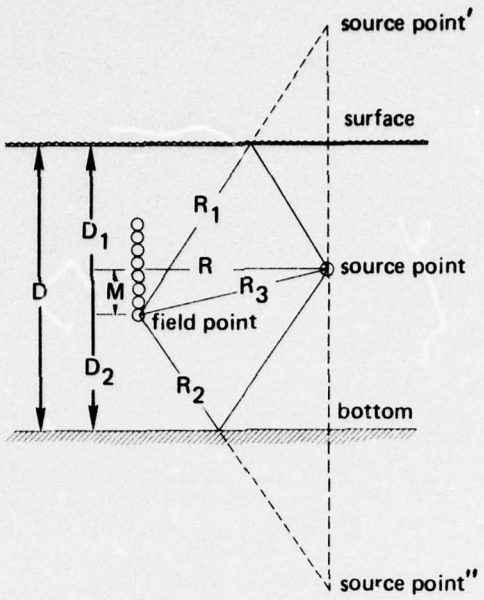

Figure 6. Image interference geometry.

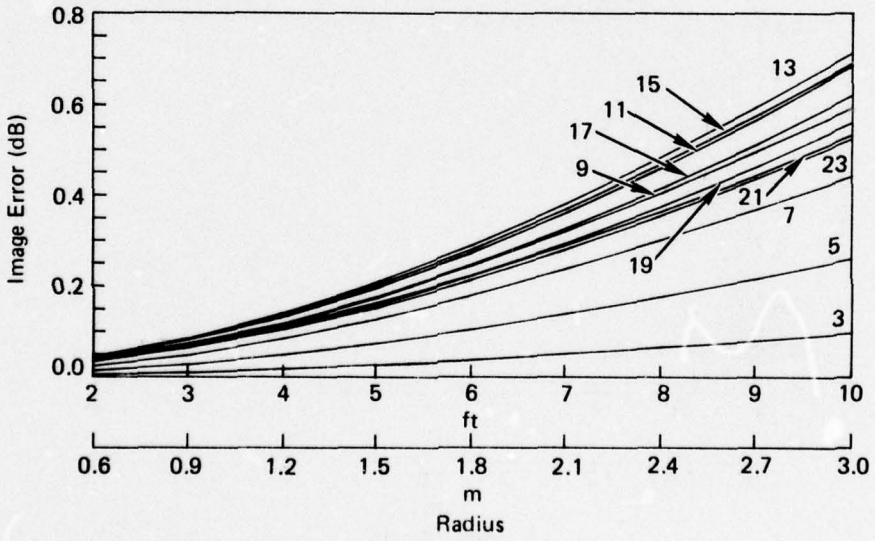

Figure 7. Image error versus radius at 1 kHz, odd layers.

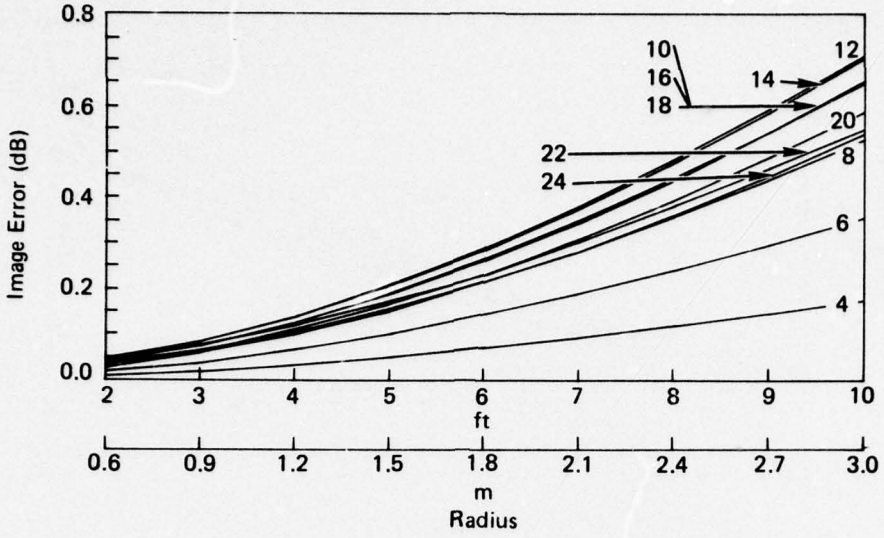

Figure 8. Image error versus radius at 1 kHz, even layers.

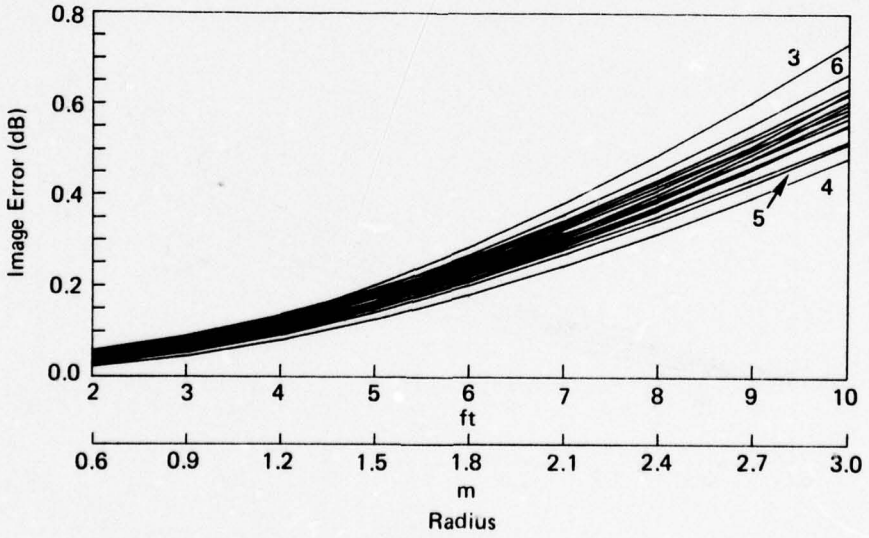

Figure 9. Image error versus radius at 5 kHz.

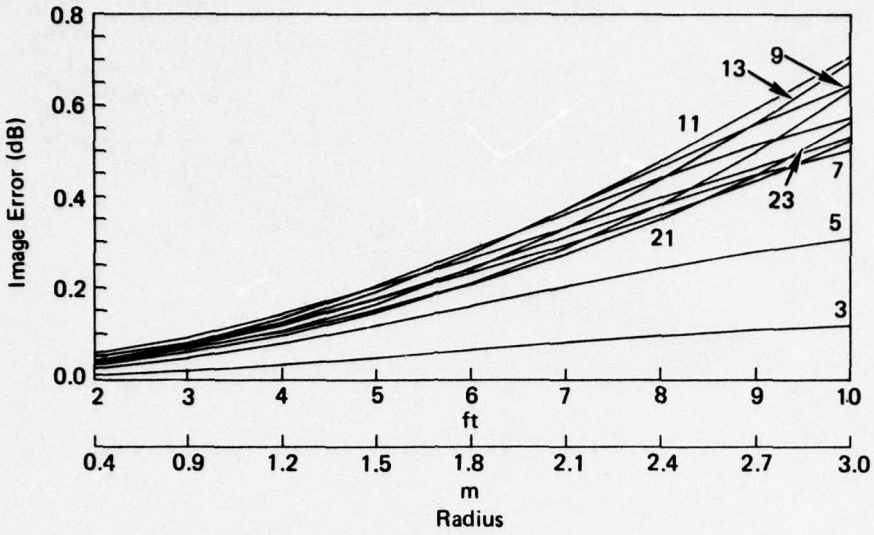

Figure 10. Image error versus radius at 10 kHz, odd layers.

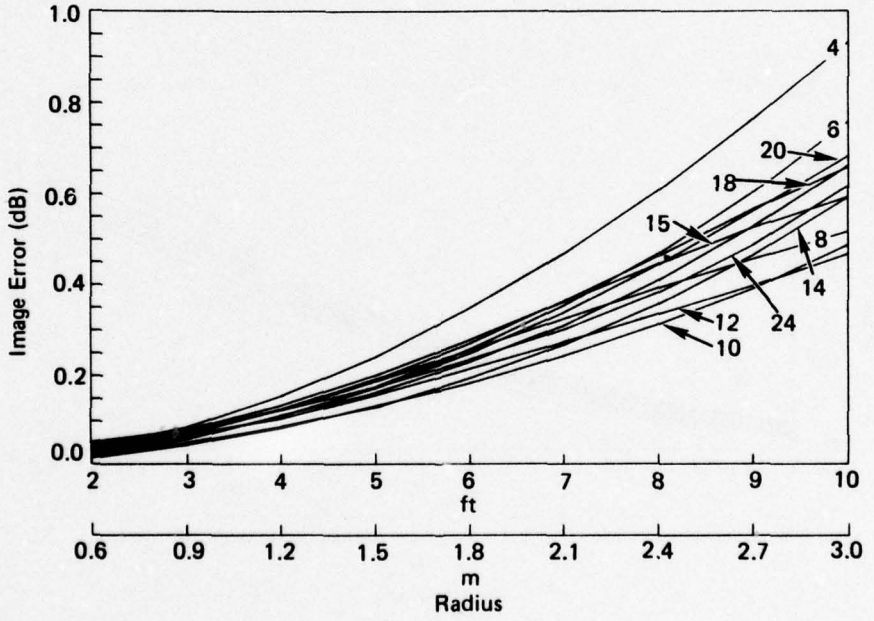

Figure 11. Image error versus radius at 10 kHz, even layers.

NUC CALIBRATION UNIT

Unit Description

The NUC hydrophone line array calibration unit (U. S. Patent No. 3,859,620, issued 5 February 1975) was constructed at NUC in January 1972 and is shown in Fig. 12.

The sketch in Fig. 13 shows the top and base (2.7-meter-diameter discs), which were made from double-thickness 1.9-cm plywood coated with three coats of fiberglass resin. The top disc has a 0.9-meter-diameter hole in the center, and the disc has been drilled for four 1.0-cm eyebolts which attach to a lifting harness. The top disc is also drilled for eight 0.6-cm eyebolts, from which the 5.5-meter, 1.3-cm line holds the calibration housing. This housing is made of heavy wire mesh which is stiff enough to retain a cylindrical shape during calibration and is opaque to acoustic transmissions within the useful frequency range.

The unit is assembled by fitting the wire mesh over the base, which is supported from the ground by wooden beams. The wire mesh is then attached temporarily to the base with large, easily removable staples. The array is then coiled within the wire mesh frame and secured with line, as shown in Fig. 14. The top support is then installed within the coiled array, preventing the top from pressing on the array during shipment to the calibration facility. The 5.5-meter support lines are attached to the wire mesh housing, the top disc is lowered within the wire frame, and staples are applied to hold the top in place during shipment (Fig. 15).

Upon the unit's arrival at the calibration facility, all staples are removed and a crane lifts out the top disc. The support cables extend until the calibration unit is lifted free of the truck bed, as shown in Fig. 12. The unit is then placed within the calibration tank and is free-floated into position for calibration.

Test Results

In this section of the report the line array calibration unit is evaluated for errors and for future users, and the results of the initial test of a standard geophysical array manufactured by the Seismic Engineering Company are presented. This array occupied 8 layers within the calibration unit.

Phase Differences for NUC Unit. Figures 16 through 19 exhibit the phase errors over the frequency range of 100 Hz to 10 kHz for 3 to 24 layers of a

line array segment within this helical wire frame. Phase errors were found to be negligible below 100 Hz for all layers, to increase with number of layers, and to increase with frequency. For the geophysical array tested, errors due to phase differences were less than –0.1 dB below 1 kHz.

Spherical Spreading for NUC Unit. Spherical spreading losses were seen to be 0.2 dB from Fig. 5, for the NUC calibration unit and geophysical array.

Image Interference for NUC Unit. Figures 20 through 23 show the loss in intensity over the frequency range of 100 Hz to 10 kHz for 3 to 24 layers of a line array segment within the NUC calibration unit. For this unit, image errors were found to increase with number of layers and with increasing frequency up to 1 kHz. Above 1 kHz the image error oscillates about 0.15 dB until the curves break up into two families of curves for the odd and even layers near 9 kHz. For the geophysical array used, image errors were approximately 0 dB up to 100 Hz and increased to 0.1 dB at 1 kHz.

Calibration Corrections for NUC Unit. Figure 24* shows the results of an 18 February 1972 measurement of the receiver sensitivity for the standard Seismic geophysical array from 40 Hz to 1 kHz. Corrections to this curve were found to be negligible, being –0.1 dB at 40 Hz and –0.2 dB at 1 kHz.

* From Naval Undersea Center report 6480, "Transducer calibration of Seismic streamers," July 1972.

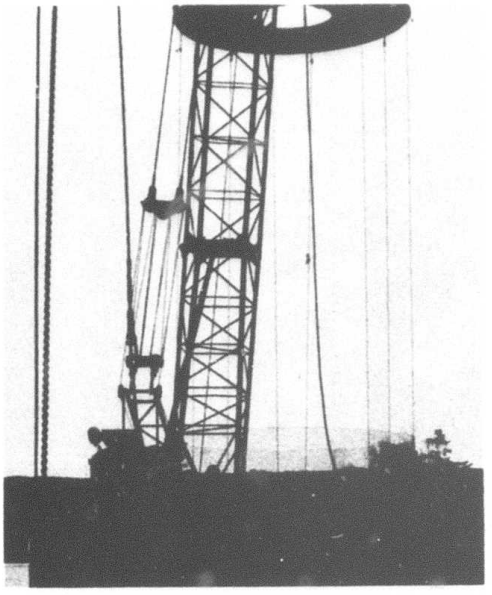

Figure 12. NUC hydrophone line array calibration unit.

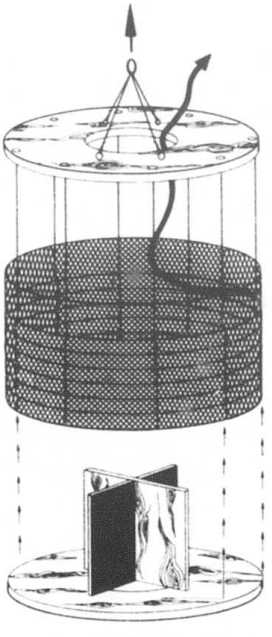

Figure 13. Sketch of NUC calibration unit.

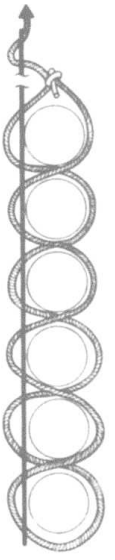

Figure 14. Method of securing array segment to wire mesh.

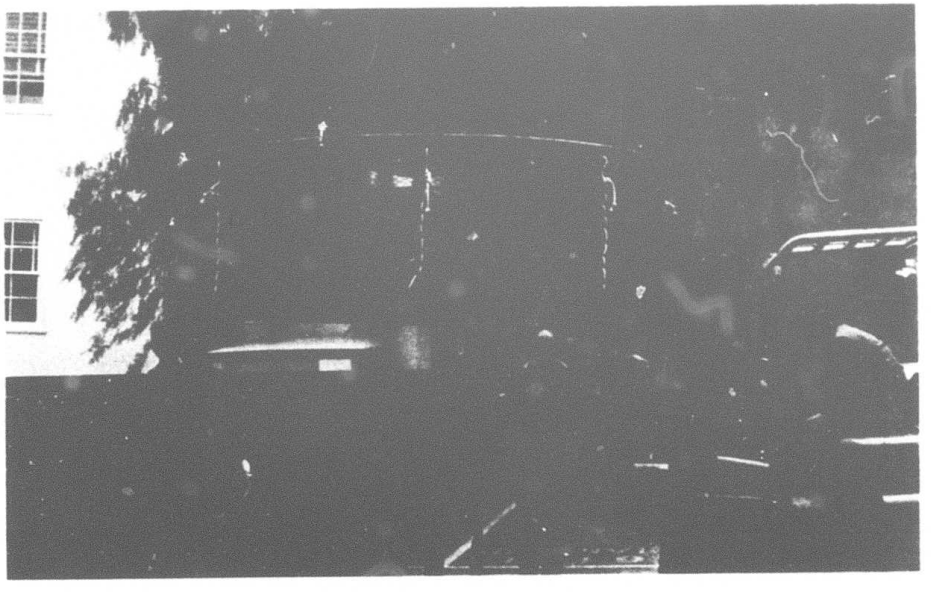

Figure 15. Calibration unit prior to shipping.

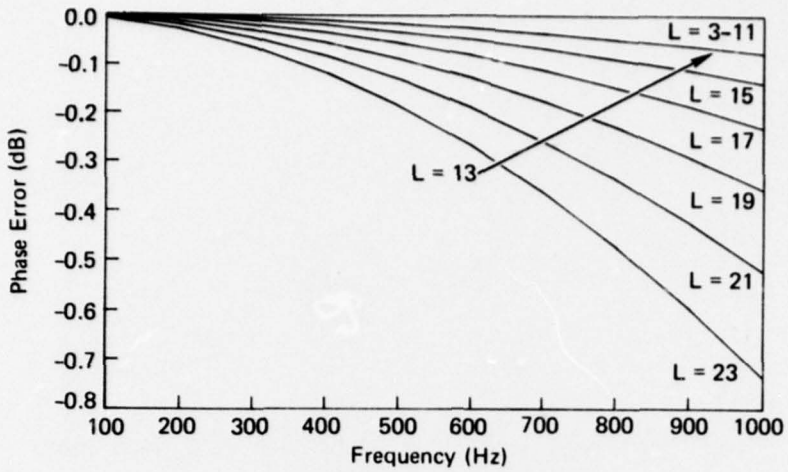

Figure 16. Phase error versus frequency, NUC unit, odd layers, 100 Hz - 1 kHz.

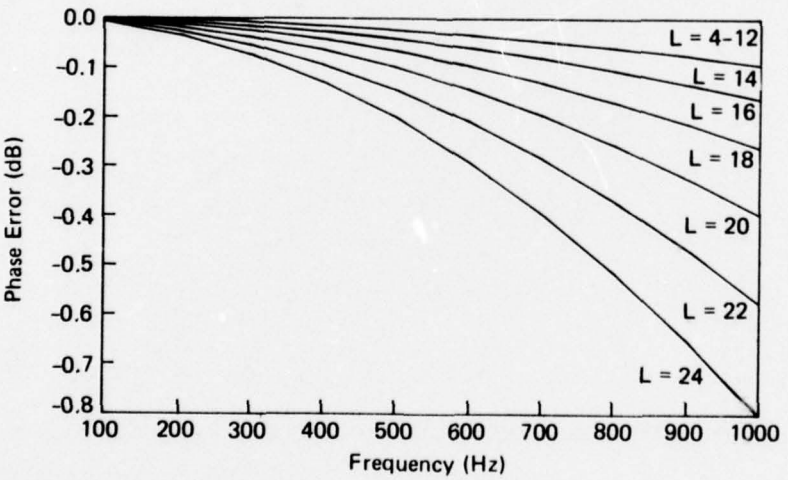

Figure 17. Phase error versus frequency, NUC unit, even layers, 100 Hz - 1 kHz.

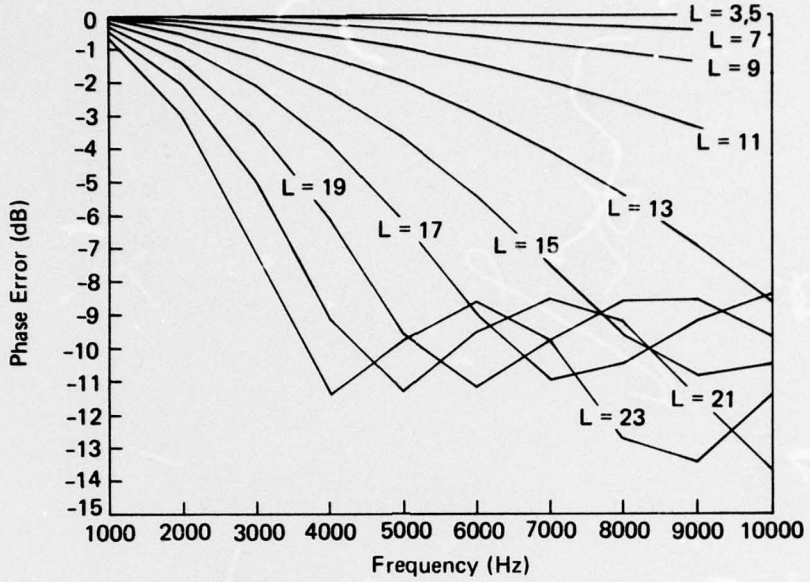

Figure 18. Phase error versus frequency, NUC unit, odd layers, 1 kHz - 10 kHz.

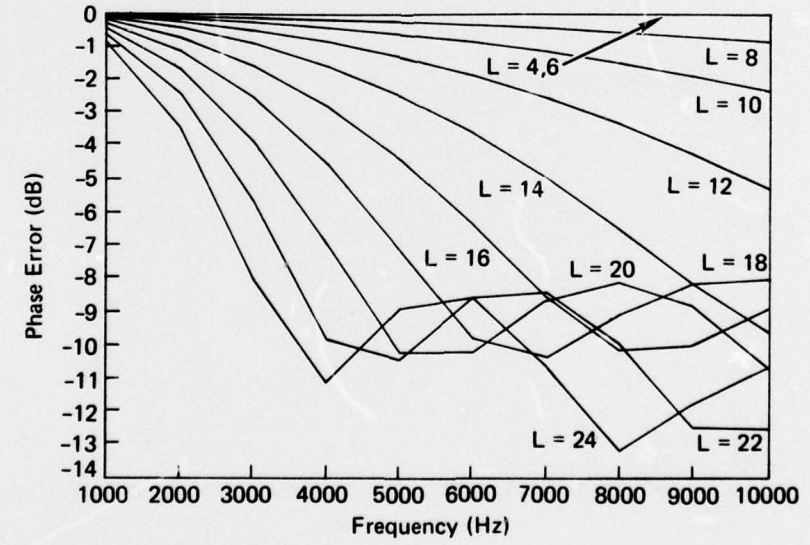

Figure 19. Phase error versus frequency, NUC unit, even layers, 1 kHz - 10 kHz.

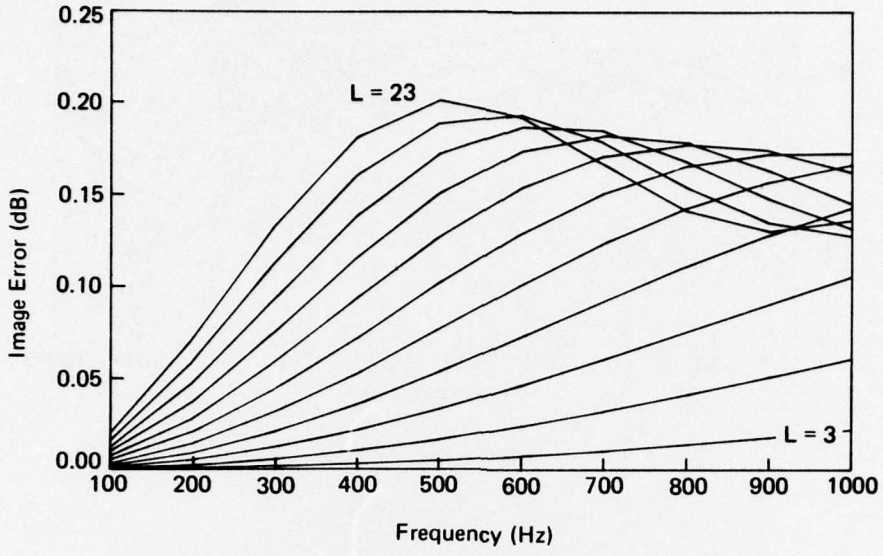

Figure 20. Image error versus frequency, NUC unit, odd layers, 100 Hz - 1 kHz.

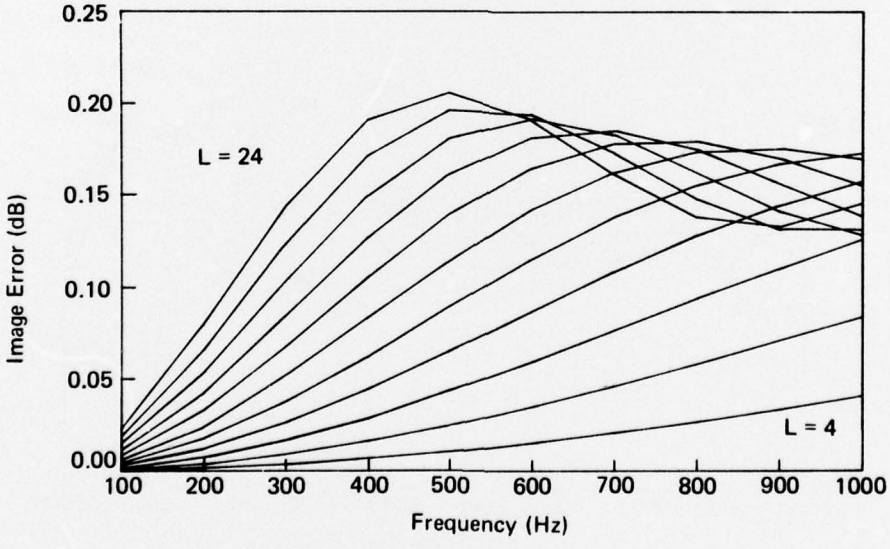

Figure 21. Image error versus frequency, NUC unit, even layers, 100 Hz - 1 kHz.

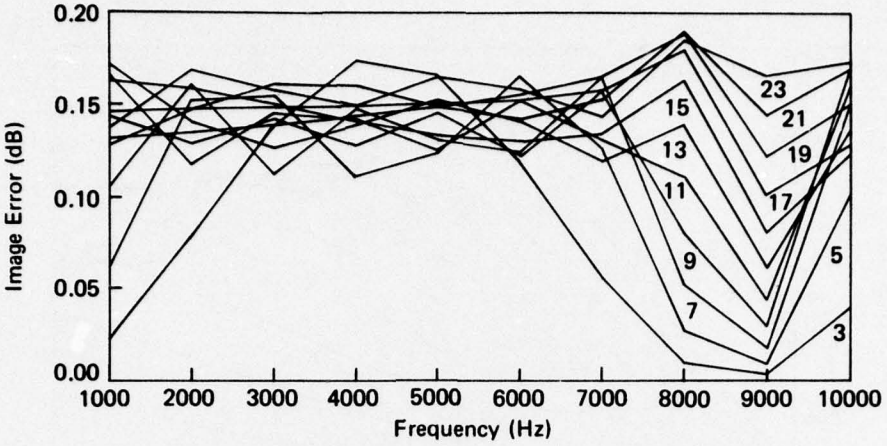

Figure 22. Image error versus frequency, NUC unit, odd layers, 1 kHz – 10 kHz.

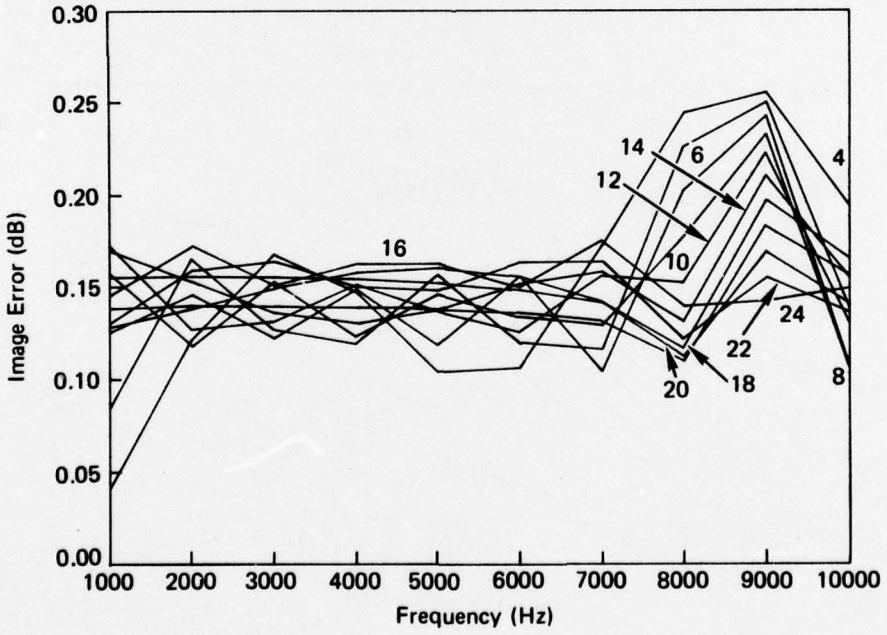

Figure 23. Image error versus frequency, NUC unit, even layers, 1 kHz – 10 kHz.

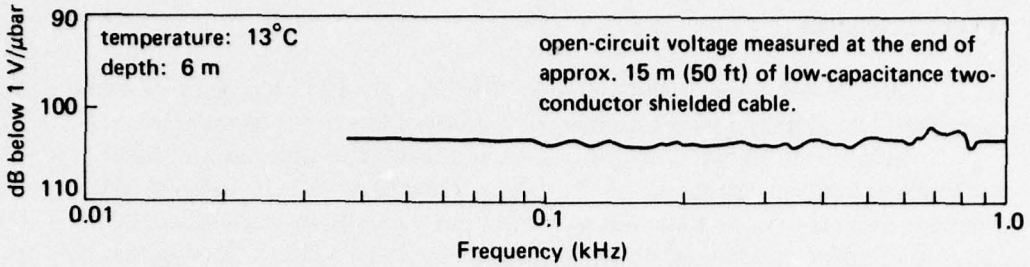

Figure 24. Measured Seismic array sensitivity.

SUMMARY OF RESULTS

1. Phase errors were found to be negligible below 100 Hz for all layers, to increase with number of layers, to increase with frequency, and to decrease with increasing radii.

2. Spherical spreading errors were found to decrease with increasing radii.

3. Image errors were found to increase with number of layers and with increasing frequency up to 1 kHz. Above 1 kHz the image error oscillates about 0.15 dB until the curves break up into two families of curves for the odd and even layers near 9 kHz. Image errors also increase with increasing radii and increasing number of layers at 1 kHz up to 12 or 13 layers, and then decrease. At 5 kHz the image error versus radii curves are fairly well grouped together, and at 10 kHz the curves diverge into two families of curves.

CONCLUSIONS

A calibration unit constructed at NUC in early 1972 has been used to successfully calibrate a large number and variety of line array segments.

It has been shown that errors associated with this unit due to phase differences between the layers of the helix are less than –0.1 dB below 1 kHz, that spherical spreading losses are no more than –0.2 dB, and that image interference effects range from 0 dB at 10 Hz to 0.1 dB at 1 kHz, indicating that no correction to the measured receiver sensitivity is required.

RECOMMENDATIONS

Considering the successful calibration measurements that have been made with this unit, it is recommended that continued use be made of this unit, or a newer version of it, for all future NUC line array segments and that similar units be used at all Navy calibration facilities.

Appendix

COMPUTER PROGRAMS FOR HP 9830

Computer programs were written in BASIC to evaluate the expressions presented in this paper. Examples are given in this Appendix.

The phase interference program requires minimal modification to run the program for either L odd or L even.

The Hewlett Packard HP 9830A Programmable Calculator, HP 9866A Thermal Line Printer, and HP 9862A X-Y Plotter were used to compute, print out, and plot the results of these programs. (For purposes of reproduction, however, it has been necessary to retype the following printouts.)

```
1 REM SPHERICAL SPREADING ERRORS
10 DIM Z[25,10]
20 D=3.5
30 FOR R=2 TO 10
40 Y0=Y8=0
50 GOSUB 320
60 NEXT R
70 SCALE 0,11,-2.7,0.1
80 XAXIS -2.6,1,2,10
90 YAXIS 2,0.2,-2.6,0
100 LABEL (*,2,1.7,0,8/11)
110 FOR X=2 TO 10
120 PLOT X-0.3,-2.7,1
130 CPLOT 2,-0.3
140 LABEL (150)X
150 FORMAT F3.0
160 NEXT X
170 LABEL (*,2,1.7,0,8/11)
180 FOR Y=-2.6 TO 0 STEP 0.2
190 PLOT 0,Y,1
200 CPLOT -2,0.1
210 LABEL (220)Y
220 FORMAT F11.1
230 NEXT Y
240 FOR L=3 TO 24
250 PEN
260 FOR R=2 TO 10
270 PLOT R,Z[L,R]
280 NEXT R
290 NEXT L
300 LETTER
310 STOP
320 M=3
330 FOR G=1 TO 2
340 K=1
350 FOR L=M TO (M+21) STEP 2
360 A0=(L-1)*D/24
370 P0=SQR(A0*A0+R*R)
380 IF (L/2-K)<0.7 THEN 450
390 Y0=Y0+1/P0
400 R0=SQR((D*D/576)+R*R)
410 A=(1+R0*Y0)/(1+K)
420 IF A>1 THEN 500
430 Z[L,R]=20*LGT(A)
440 GOTO 510
```

```
450 Y8=Y8+1/P0
460 B=(1+2*R*Y8)/(1+2*K)
470 IF B>1 THEN 500
480 Z[L,R]=20*LGT(B)
490 GOTO 510
500 Z[L,R]=0
510 WRITE (15,520)L,R,Z[L,R]
520 FORMAT 2F10.1,F16.1
530 K=K+1
540 NEXT L
550 M=M+1
560 NEXT G
570 RETURN
580 END


1 REM PHASE INTERFERENCE ERRORS
10 DIM V[25],P[25,10]
20 C=5000
30 D=3.5
40 R=4.5
50 F=100
60 FOR N=1 TO 10
70 S0=C0=0
80 W=2*PI*F/C
90 GOSUB 370
100 F=F+100
110 WRITE (15,520)
120 NEXT N
130 SCALE 0,1100,-1.1,0.1
140 XAXIS -1,100,100,1000
150 YAXIS 100,0.1,-1,0
160 LABEL (*,2,1.7,0,8/11)
170 FOR X=100 TO 1000 STEP 100
180 PLOT X-100,-1.1,1
190 CPLOT 2,-2
200 LABEL (280)X
210 NEXT X
220 LABEL (*,2,1.7,0,8/11)
230 FOR Y=-1 TO 0 STEP 0.1
240 PLOT 0,Y,1
250 CPLOT -2,0.1
260 LABEL (261)Y
261 FORMAT F4.1
270 NEXT Y
```

```
280 FORMAT F8.0
290 L=23
300 F=100
310 PEN
320 FOR N=1 TO 10
330 PLOT F,P[L,N]
340 F=F+100
350 NEXT N
351 LETTER
360 STOP
370 K=1
380 FOR L=3 TO 23 STEP 2
390 A0=(L-1)*D/24
400 P0=SQR(A0*A0+R*R)
410 X0=W*(P0-R)
420 C0=C0+COS(X0)
430 S0=S0+SIN(X0)
440 T0=SQR(C0*C0+S0*S0)
450 V[L]=ABS((1+2*T0)/(1+2*K))
460 IF V[L]<0.0001 THEN 480
470 P[L,N]=20*LGT(V[L])
480 GOTO 500
490 P[L,N]=-80
500 WRITE (15,510)L,F,V[L],P[L,N]
510 FORMAT 2F10.1,7X,E9.2,F13.1
520 FORMAT /
530 K=K+1
540 NEXT L
550 RETURN
560 END


10 REM IMAGE INTERFERENCE ERRORS
20 DIM V[25],P[25,10]
30 C=5000
40 D=3.5
50 R=4.5
60 R9=R*R
70 R0=SQR(R9+1296)
80 I0=1
90 F=100
100 FOR N=1 TO 10
110 S0=C0=I1=0
120 W=2*PI*F/C
130 GOSUB 440
```

```
140 F=F+100
150 WRITE (15,710)
160 NEXT N
170 SCALE 0,1100,-0.05,0.32
180 XAXIS 0,100,100,1000
190 YAXIS 100,0.05,0,0.3
200 LABEL (*,2,1.7,0,8/11)
210 FOR X=100 TO 1000 STEP 100
220 PLOT X-40,0,1
230 CPLOT 0,-1
240 LABEL (330)X
250 NEXT X
260 LABEL (*,2,1.7,0,8/11)
270 FOR Y=0 TO 0.3 STEP 0.05
280 PLOT 0,Y,1
290 CPLOT -4,0.1
300 LABEL (310)Y
310 FORMAT F6.2
320 NEXT Y
330 FORMAT F5.0
340 FOR L=4 TO 24 STEP 2
350 F=100
360 PEN
370 FOR N=1 TO 10
380 PLOT F,P[L,N]
390 F=F+100
400 NEXT N
410 NEXT L
420 LETTER
430 STOP
440 S=2
450 FOR Q=1 TO 2
460 I1=0
470 FOR L=S TO (S+23) STEP 2
480 M1=(L-1)/2
490 M=-M1*D/12
500 R7=R9+M*M
510 A=SQR(R7)
520 FOR G=1 TO 2
530 R1=SQR(R9+(36-M)*(36-M))
540 R2=SQR(R9+(36+M)*(36+M))
550 T1=(R1-A)
560 T2=(R2-A)
570 U=((2*R7)/(R1*R2))*(COS(W*T1)*COS(W*T2)
    +SIN(W*T1)*SIN(W*T2))
```

```
580 I1=I1+1+R7*(1/(R1*R1)+1/(R2*R2))+2*A*(COS(W*T2)
    /R2-COS(W*T1)/R1)-U
590 M=-M
600 NEXT G
610 IF Q=1 THEN 640
620 V[L]=ABS((I1+I0)/L)
630 GOTO 650
640 V[L]=ABS(I1/L)
650 IF V[L]<0.0001 THEN 680
660 P[L,N]=10*LGT(V[L])
670 GOTO 690
680 P[L,N]=-80
690 WRITE (15,700)L,F,V[L],P[L,N],R1,R2,A,U,I1
700 FORMAT 2F8.1,3X,E9.2,F10.1,3F8.1,2F8.3
710 FORMAT /
720 NEXT L
730 S=S+1
740 NEXT Q
750 RETURN
760 END
```